

Article

The Environmental Control of Historic Arab Baths: A Thermodynamic Simulation of the Hernando de Zafra Baths in Granada

Santiago Tormo Esteve ¹, Eduardo Loma-Ossorio Blanch ², Fernando Vegas López-Manzanares ^{3,*} and Camilla Mileto ³

- ¹ Departamento Construcciones Arquitectónicas, Universitat Politècnica de València, 46022 Valencia, Spain; santores1@gmail.com
- ² Escuela de Doctorado, Universitat Politècnica de València, 46022 Valencia, Spain; edlobla@gmail.com
- ³ Departamento Composición Arquitectónica, Universitat Politècnica de València, 46022 Valencia, Spain; cami2@cpa.upv.es
- * Correspondence: fvegas@cpa.upv.es; Tel.: +34-669847292

Abstract: The Arab baths of Hernando de Zafra, popularly known as Casa de las Tumbas, are found at the intersection of calle Elvira and calle San Andrés in the historic centre of Granada (Spain). This article presents a thermodynamic study of the environmental operation of this complex of Arab baths, which has a furnace and hot, warm, and cold rooms, as well as auxiliary adjoining spaces and annexes. Computer models are used for the finite element analysis of the fluid dynamics for the process of lighting the furnace and subsequently diffusing the temperature, and smoke is expelled through the chimneys. The FDS software used—verified and validated by the NIST—processes the conditions for lighting the furnace and the thermal transmission of the generated heat to the different rooms in the building. This is the first case of this software being used for an analysis of the ancient Arab baths. The results show the global thermal behaviour, and the conclusions establish the temperatures reached inside the rooms and the thermal energy contributions needed to reach these temperatures.

Keywords: Arab baths; temperature; furnace; diffusion; environmental control



Citation: Tormo Esteve, S.; Loma-Ossorio Blanch, E.; Vegas López-Manzanares, F.; Mileto, C. The Environmental Control of Historic Arab Baths: A Thermodynamic Simulation of the Hernando de Zafra Baths in Granada. *Buildings* **2024**, *14*, 39. <https://doi.org/10.3390/buildings14010039>

Academic Editor: Md Morshed Alam

Received: 12 October 2023
Revised: 12 December 2023
Accepted: 14 December 2023
Published: 22 December 2023



Copyright: © 2023 by the authors. Licensee MDPI, Basel, Switzerland. This article is an open access article distributed under the terms and conditions of the Creative Commons Attribution (CC BY) license (<https://creativecommons.org/licenses/by/4.0/>).

1. Introduction

In general, Arab baths follow a standard layout sequence consisting of three main rooms: a cold room, warm room, and hot room, known in Arabic as *bayt al-barid*, *bayt al-wastani*, and *bayt al-sajun*, respectively. Sometimes, this layout might also include a vestibule or *bayt al-maslaj*, a space for dressing and undressing, as well as other essential service rooms, such as furnace and fuel storerooms. In the historic centre of Granada, at the intersection of calle Elvira and calle San Andrés, we find the Arab baths of Hernando de Zafra, which have no record of their original Arabic name, but are popularly known as Casa de las Tumbas. In addition to the baths, furnace, and hot, warm, and cold rooms, the former vestibule can be made out in the back courtyard of the complex, which is now in ruins. Although this article focuses on the thermodynamic operation of the baths, a brief summary of their history is presented below.

1.1. State-of-the-Art Software

Research based on the software application of computational techniques to the study of the fluid dynamics of old construction is scarce. In this study, the methodology followed was developed by the Fire Research Division, Engineering Laboratory, Gaithersburg, Maryland; Aalto University, Espoo (Finland); and the Fire Safety Research Institute, UL Research Institutes, Columbia, Maryland [1]. This simulation software was chosen because

it considers the orthogonal geometry and allows for a simplified handling of the equations, with shorter processing times than other software.

Studies performed with modelling and simulation tools make it possible to research different situations that cannot be verified in a real-life setting. This can be clearly seen in the research by Qi, D. et al. [2], which tested the position of the upper opening of a system aiming to improve smoke extraction when a fire is lit.

Other finite element calculation programs involve longer calculation times. Numerous hypotheses, including the research presented by Dufour in 2006, have been proposed, given that the volumes of the buildings studied are complex [3]. Had these programs been used here, the calculation time would have increased ten-fold. However, the publications we consulted used tools such as ANSYS FLUENT, which is also based on computational fluid dynamics (CFD). This allows for more precise calculations with slower data processing, as well as a final analysis treatment for more complex geometries, as described by Gagliano [4] (pp. 704–715). Basaran and Ilken [5] used these programs on a smaller scale to establish the energy efficiency of a radiant floor system compared to that of a wall heating system.

Similar studies following similar methods can also be found, including the research by Potier and his team [6] (pp. 117–128), which showcased the importance of computational techniques applied to different hypotheses concerning archaeological remains. Orehounig [7] (pp. 2442–2448) studied energy transmission in traditional baths, while Oetelaar [8] (pp. 59–66) [9] (pp. 1–6) examined the results of the application of computational methods to the hot rooms of the Roman baths.

Finally, three studies have verified and largely completed a CFD for use in the simulation of a wide range of scenarios. These include complex geometries, multiple lengths/timescales, and multiphysics simulations (i.e., turbulence, combustion, heat transfer, soot generation, solid pyrolysis, flame spread, and liquid evaporation), which cannot be studied easily using analytical solutions and zone models. The first of these is the article by Maragkos and Beji [10], which focused on convection and reviewed the most widely used approaches to fire-driven flows for modelling convective heat transfer using CFD and Large Eddy Simulations (LES). The second is the End-of-Master's thesis by Bueno [11], which examined the effect of variations in the size, distribution, and location of the vents on the results, in order to establish the overall effect of ventilation on the final results when a fire is active. Finally, the third study referenced is that by Also-Moya [12], which detailed several tests carried out for the validation of computational programs.

As seen in the existing literature that has been consulted, the use of computational methods is widespread for observing the behaviour of historic buildings. However, this has never been performed for Arab baths with layouts as unique as that of Hernando de Zafra. Given the extensive presence of this type of bath in the Iberian Peninsula, applying this technique is vitally important when seeking to draw conclusions which may be of use for studying similar buildings.

1.2. Objectives

The main objective of this study is the reconstruction of the architectural model based on the data obtained from the surviving archaeological remains. The thermal operation of the hot rooms, as well as the openings and ducts in the walls, will be examined on the basis of these data.

The first objective is to ascertain whether the conduits in the walls between the warm and hot rooms are large enough to provide the flow needed to warm the hot room to an optimal temperature, while ensuring a suitable heat for the fire.

The second objective is to confirm whether heat is being uniformly distributed across the hot room floor and whether the structures supporting this floor can guarantee uniform temperatures.

The third objective is to confirm whether the light shafts on the roof are functional, and whether these can provide ventilation or only light.

Finally, the fourth objective is to confirm heat transmission by hot air convection through the communicating doors of the other rooms in the baths.

2. History

These baths were first mentioned briefly in a 16th-century document on pious endowments linked to the surroundings of the church of San Andrés [13]. Following the Christian conquest, this property may have been ceded directly by the Catholic kings to their secretary, Hernando de Zafra, Lord of Castril. The name Casa de las Tumbas, a possible reference to the shape of the cloister vaults as seen from the exterior, dates from the early 18th century, and is mentioned in the *Manual del artista y del viajero en Granada*, published in the mid-1800s [14]. This work also described the deplorable condition of the building, which still retained its walls and vaults but had been transformed, adapted, and reused as housing, and was also frequently mentioned in later decades. The most detailed description can be found in *Granada. Guía Artística e Histórica de la ciudad* (1961), which notes that the vaults, although abandoned and dirty, were in good condition [15]. Their condition was further described during the rest of the 20th century, as a process of recovery began to take shape. The housing was expropriated and detailed archaeological and stratigraphic studies were carried out on the remains. Subsequently, parts of the complex, including some of the 19th- and 20th-century dwellings, were either demolished or shored up. This project of the consolidation of the baths also included a thermodynamic study of their operation, which is presented below.

2.1. Location

These baths, set in a built-up area of the former medina, were influenced by the existing urban layout and its irregularities. This could potentially complicate the understanding of the aspects of these spaces that were key to the building's operation. Access to the building was probably the same as that currently used to enter the archaeological complex. This is through calle San Andrés, opposite the church of the same name, and built on a site previously occupied by a mosque. The users of the baths probably entered via a corridor on the left that, after a bend, led to the entrance to the cold room through a side chamber. This bend probably provided protection for the spaces requiring optimal thermal control, while also acting as a vestibule, given the lack of a specific room for this purpose.

Unlike the other two rooms—the warm room and hot room—the rectangular cold room may have been accessed via a corridor on the shorter side, possibly determined by the existing urban layout. The baths may also have been accessed through the courtyard and possibly linked to the nearby Plaza de los Naranjos behind the mosque, a more sheltered spot within the urban epicentre of Elvira. Courtyard access is a feature of other Arab baths, such as that of El Bañuelo, also in Granada.

2.2. Hydraulic Supply

As baths and mosques are two types of buildings which require a constant flow of water, it seems logical for these to be found close together [16] (p. 6). Water was also needed for ablutions in the baths in preparation for prayer in the mosque. The supply of water to the baths was generally guaranteed by the network of irrigation ditches in the city, as seen in the Hernando de Zafra baths. Whenever the surrounding conditions prevented this, water was taken from wells, as in the case of the Dar al-Arusa baths near the Generalife, where there is evidence of a wheel which supplied water extracted from a well.

There is speculation as to whether the location of the baths was due to the previous presence of an irrigation ditch, or whether a channel was built to supply the baths and mosque with water. Given the prominence of calle Elvira within the city, it appears that the baths were built where there was already a constant supply of water, possibly from a channel from the Axares irrigation ditch [17] (pp. 76–77). This ditch, also known as San Juan, begins at a fork in the Acequia de la Ciudad irrigation channel, with water from the river Darro. It seems possible that the Hernando de Zafra baths were connected to this

water flow. The site of the baths also displays slight differences in its level, using gravity to facilitate the supply and drainage of water.

For this building floor plan, the cold, warm, and hot rooms account for 350 m² of the surface area. The remaining rooms (vestibule, storage areas, and furnace) add approximately 130 m² to the surface area. The rooms are all different heights, and the highest ceilings, 4 m, are in the warm room. Therefore, the volume of the complex almost certainly exceeded 1000 m³ (Figures 1 and 2).

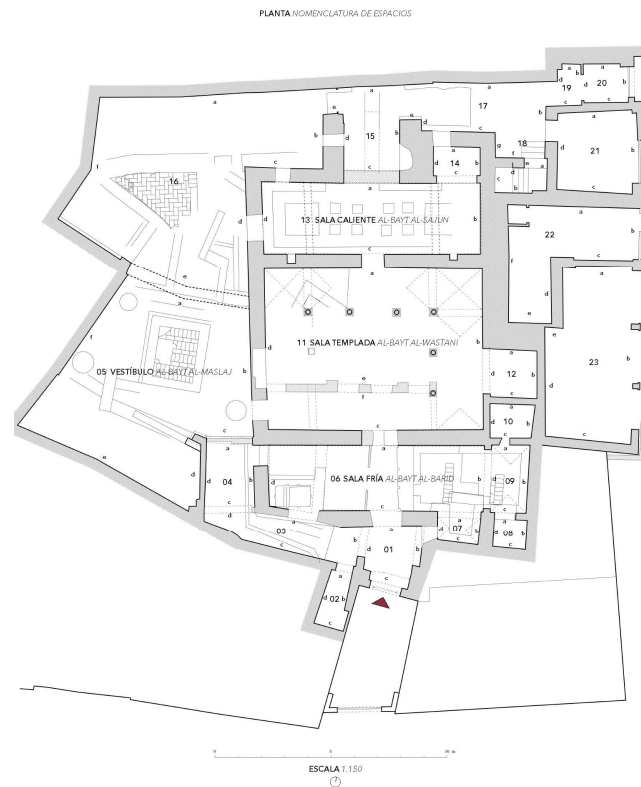


Figure 1. Building floor plan.



Figure 2. Warm room.

3. Methodology

3.1. Thermodynamic Analysis Using Computer Models

This research aims to provide a virtual reproduction of the operation of these baths following a series of hypotheses. The initial comprehensive data collection on the building helped to complete our information about the details of the different rooms. It offers an interpretation of the openings, pipes, and any imprints, providing information about the elements and a more accurate representation of how the baths could have been built in order to operate correctly. Once the architectural data were analysed and transferred to a computer model, all the potential scenarios were reproduced.

Two computer programs for the finite element analysis of fluid dynamics were used to analyse the simulation of the furnaces in operation at the baths. Given that the principles of thermodynamics and fluid dynamics do not change, the main challenge to applying this process to this type of complex is establishing the different hypotheses replicating the potential situations, and ensuring a final result that is as close as possible to reality.

Two software programs were used for all the simulations in this research:

- Fire Dynamics Simulator—FDS 6.0;
- Smokeview.

Both programs were developed by the Building and Fire Research Laboratory of the NIST (National Institute of Standards and Technology) [1], in collaboration with VTT Building and Transport (Finland) and other prestigious institutions, adding further credence to the validity and effectiveness of the calculations carried out here.

The Fire Dynamics Simulator—FDS 6.0 software uses a simulation model and CFD equations to provide solutions to situations generated by conduction, radiation and, above all, convection. The software mostly uses the Navier–Stokes equations, focusing on the calculation of low-velocity thermal flow situations, such as those of the movement of hot air and smoke, as well as those of thermal effect flows. This software analyses a model as a volume made up of cells in three directions, to which physical properties (such as density) and thermal properties (conductivity and specific heat) are added. The data consider the cells as solid bodies (described in the program as obstructions), whose properties are entered to define the nature or construction material (stone, brick, water, etc.) of each cell. In the case of air-filled cavities or openings, the cell data are entered in the same way, simply noting that the cell in question corresponds to an “empty” solid containing air, and recording its properties in the same way as for the solid cells.

Another key element of the program is the model used to examine the turbulence which occurs in the limits of pyrolysis between the flames and the air. In FDS, the LES model is used to analyse turbulence, showing non-stationary patterns in constant change, and predicting the vertical movement caused by convection and conduction in the cavities [18].

For the solid elements, the thermal properties of each type of body are entered, and the program calculates the results below for each time interval:

- The temperature at the cell limits;
- The heat flow due to convection and radiation;
- The combustion speed.

For the elements that are considered to be empty (i.e., filled with gas), the aspects identified by the program include:

- The temperature of the gas (in this case, air);
- The direction and speed reached by the gas due to convection.
- The following values are also obtained for the entire system model:
- The HRR (heat release rate);
- The behaviour of temperature and wind observation points based on temporal evolution;
- The mass and energy flows through the openings and spaces generated.

The program completes a complex mathematical operation in which all the thermodynamics equations affect the situations of the individual cells, considering the finite and

homogeneous elements, and progressively implementing the results from the adjoining cells. In the final stage of the calculation, the result of the proposed hypothesis is based on the properties of the individual cells and the boundary conditions entered into the model. The amount of calculations and equations varies depending on the size and number of the cells. The smaller the size and number of the cells, the more precise the results, although some studies have shown that this depends more on the geometry of the model than on the actual size of the cells [3] (p. 46).

The model used is based on the equations for the conservation of mass, momentum, and energy for a Newtonian fluid. The same equations are used in the rest of the CFD models.

The equation for mass conservation is expressed in terms of density:

$$\frac{\partial \rho}{\partial t} + \nabla \cdot \rho \mathbf{u} = \dot{m}_b'''$$

The equation for the conservation of momentum:

$$\frac{\partial}{\partial t}(\rho \mathbf{u}) + \nabla \cdot \rho \mathbf{u} \mathbf{u} + \nabla p = \rho \mathbf{g} + \mathbf{f}_b + \nabla \cdot \boldsymbol{\tau}_{ij}$$

The equation for the conservation of energy:

$$\frac{\partial}{\partial t}(\rho h_s) + \nabla \cdot \rho h_s \mathbf{u} = \frac{Dp}{Dt} + \dot{q}''' - \dot{q}_b''' - \nabla \cdot \dot{\mathbf{q}}''' + \varepsilon$$

The calculations generate numerous parametric files whose size depends on the time interval and on the number and size of the cells considered. All the data were processed using Smokeview (SMV) in order to ensure a clearer definition of the final behaviour. As the calculation data obtained with this software can be viewed in 3D, the information can be edited and plans can be generated to interpret the points where information is requested and to analyse their evolution throughout the process. The vector plans can, therefore, be visualised, showing the direction and speed of the hot air and carrying out occasional temperature readings for individual points on the surfaces, as well as fluid temperature readings for any point of the model, etc.

The model assessment process is composed of two parts: verification and validation. The process of verification [19] is used to confirm that the solution of the equations used is correct. However, verification does not imply that the governing equations are appropriate, only that they are resolved correctly. Validation [20] is used to determine the suitability of the equations used in the mathematical model for the reproduction of the physical phenomena occurring in reality. In general terms, validation is the comparison of the computer model results and the experimental results.

The differences which cannot be explained in terms of numerical errors in the model or uncertainty in the measurements are attributed to the assumptions and simplifications of the physical model.

Validations are crucial for establishing the acceptable uses and limitations of a model. Throughout its development, FDS has undergone several evaluations by the NIST, as well as by specialists, universities, and other bodies. The Validation Guide reflects the continued efforts on the part of the NIST and other bodies to evaluate FDS as new capabilities are added. To date, most of this work has focused on this model's ability to predict the transport of heat and flame products by a fire throughout a space, as well as the interaction of the solid elements which make it up.

The default FDS turbulence model, optimised for fires in buildings with a fire-driven fluid flow, was used for the simulations here. In this case, the LES (Large Eddy Simulation) was preferable to the DNS (Direct Numerical Simulation), as the excessively small cell size required would not have been viable for studying volume on the scale of the baths in Granada.

Since the validation guide (Fire Dynamics Simulator Technical Reference Guide, Volume 3: Validation) lists numerous studies that have been conducted on spaces with similar measurements, this model is considered appropriate for the proposed study.

Numerous studies have applied these programs for examining the behaviour of fire and smoke. One example of this is the study by Jen-Hao Chi [21], who used FDS + EVAC to ascertain the behaviour of the hotel fire responsible for the highest death toll in the history of Taiwan. Another example is the article by Sgu, C. and Wang, L.L. [22], which analysed smoke and fire behaviour using FDS; this paper confirmed the effectiveness of the procedure for assessing the spread of smoke in very tall buildings.

3.2. Architectural Model

For the architectural model reproduction, the geometry was simplified, taking into account the requirements for the heat transmission calculation in both the solid and fluid materials (Figure 3):

- The heights of the rooms and of the hypocaust connected to the furnace;
- The measurements of the walls and the load-bearing elements of the hypocaust floor;
- The composition of the different building layers, defining material typologies, and the thicknesses of their constructions;
- The separations between and the distances of the openings and pipes;
- The location of the heat source (furnace);
- The communication between rooms.

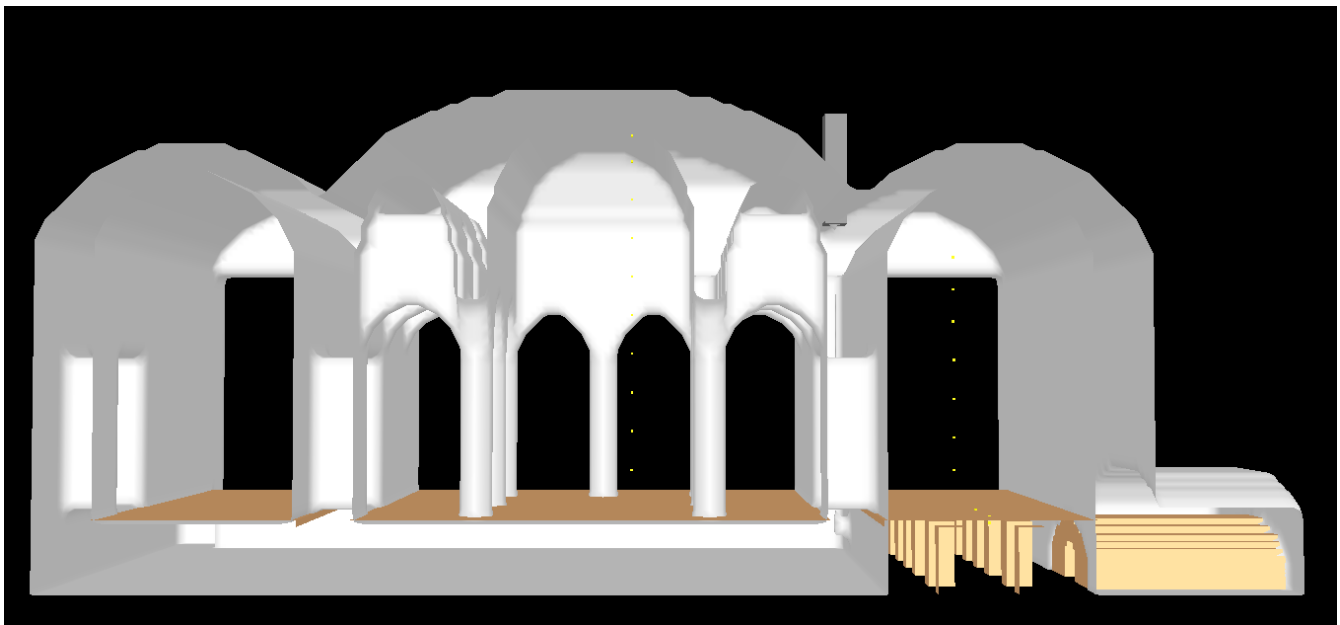
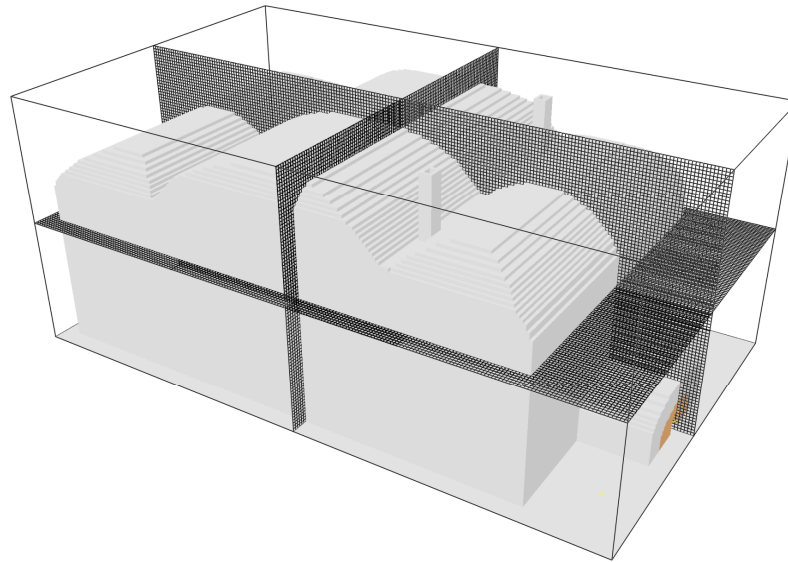
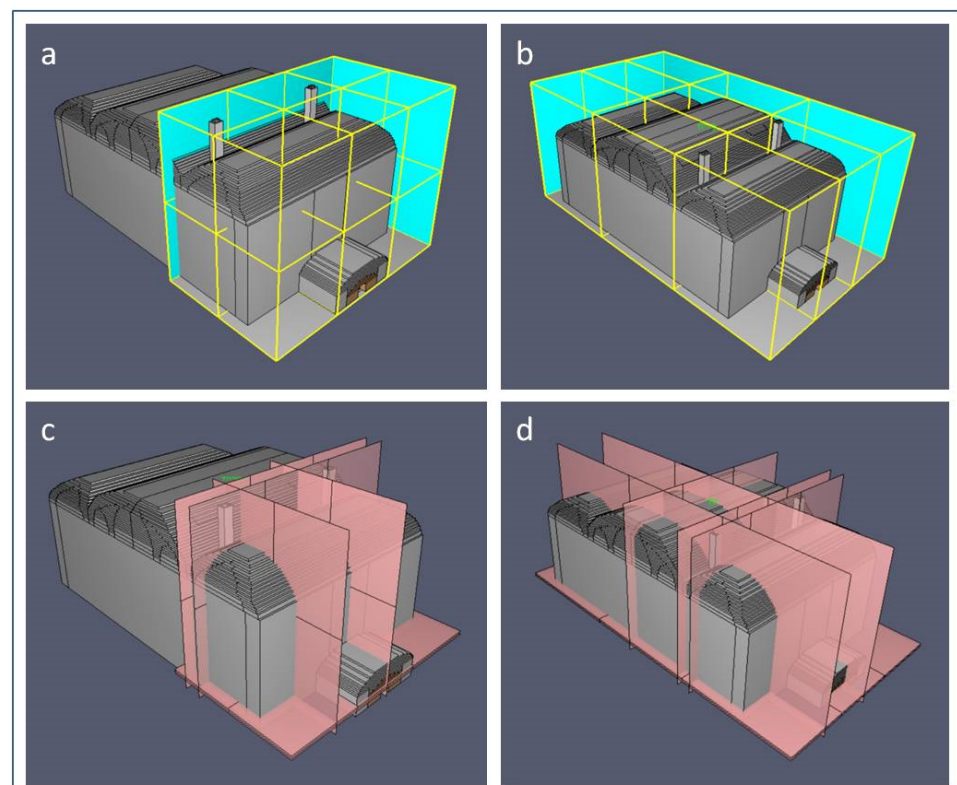


Figure 3. Computer model. The yellow dots are virtual observation points for temperature and velocity inside the rooms of the baths.

The geometry of the complex was reproduced as a 3D mesh of cubic cells with 10 cm sides in a model showing the shapes of the vaults and walls of the building. The thermodynamic equations were applied to transmit the results between the individual 3D cells and to provide a combined solution to the final situation generated. The cell measurements established were as close as possible to the building size, and the calculations performed were in line with similar, previous calculations [23]. The application of this 3D mesh produced a model consisting of 2,332,800 cells (Table 1, Figures 4 and 5).

Table 1. Graph showing simulation configurations.

Configuration of Simulations					
Simulations	Cell Size	Number of Meshes	Total Cells	Simulated Hours	Simulated Seconds
1. Hot room	10 cm	12	777,600	115	7750
2. Complete geometry	10 cm	9	2,332,800	132	1000

**Figure 4.** Schema of the 3D mesh. A model consisting of 2,332,800 cells.**Figure 5.** Schema of the 3D mesh of the baths: (a) configuration of 12 meshes for multi-processing in the hot room; (b) configuration of 9 meshes for multi-processing in the complete geometry; (c,d) configuration of temperature and flow velocity plans.

After the 3D reconstruction of the geometry of the baths and the introduction of materials for each of the enclosures, performed as close as possible to reality, a fire was placed in the outer area of the furnaces in the simulations. Air characteristics were used to define the openings, and the data for the individual construction materials used in the structure were entered. This geometry was applied to the planes to fit within a 10×10 cm cubic mesh, which is the minimum size dimension that could be used for the existing openings of the building.

Both the height of the entry flues to the chimneys within the hypocaust and the interior section of the two exit chimneys were considered to be of critical importance. The software takes into account the rounding of corners, so that the wind path does not follow the corners of the cubic meshes but is simplified by joining the ends.

The boundary conditions are the physical and atmospheric parameters that define the exterior of the simulated space at the beginning of the simulation. The outer limits of the model are those of an open space with the following characteristics:

- Exterior temperature, 25 °C;
- Relative humidity, 40%;
- Gravity, 9.81 m/s²;
- Initial wind, 0 m/s;
- Atmospheric pressure, 101,325 Pa.

In this case, the conditions selected were the default conditions provided by the model.

The lower section of the enclosure or the base of the model is a limestone slab 40 cm thick, with the following thermal properties:

- Thermal conductivity, 2.1 W/(m² K);
- Specific heat, 4.2 kJ/(kg K);
- Density, 2400 kg/m³;
- Emissivity, 0.9.

The following properties of the materials were considered for the calculation of the heat transfer (Tables 2 and 3, Figure 6).

Table 2. Material properties.

Material Properties					
Material	Units	Limestone	Clay Brick	Gypsum	Concrete
Specific heat (c_p)	kJ/(kg·K)	0.712	0.879	0.837	0.669
Density (ρ)	kg/m ³	2400	1460	1440	1920
Conductivity (λ)	W/(m·K)	2.104	1.279	0.488	0.090
Emissivity		0.9	0.9	0.9	0.9

Table 3. Location and U of constructive materials.

Constructive Element	Materials	U W/m ² K
Furnace interior	Clay brick (40 cm)	3.19
Furnace exterior	Limestone (30 cm)	7.01
Hot room floor	Clay brick (10 cm) Concrete (10 cm)	0.84
Hypocaust pillars	Clay brick (20 cm)	6.39
Cold room floor	Clay brick (10 cm) Limestone (40 cm)	3.84
Interior enclosures	Gypsum (2 cm) Clay brick (30 cm)	3.51
Interior pillars	Gypsum (2 cm) Clay brick (30 cm)	3.51
Roof	Concrete (10 cm) Clay brick (30 cm)	0.74
Exterior walls	Gypsum (2 cm) Limestone (40 cm)	4.16

Control points were installed in each room in the virtual model to obtain the data and results showing the evolution of the entire process. The conclusions could be used to

establish fluid temperatures (Figure 7), directions, and speeds. In combination with the information obtained, these virtual observation points provided the following parameters:

- Surface temperatures;
- Isosurfaces of temperatures at 30, 40, and 50 °C;
- Temperature plans inside the rooms;
- Flow speed plans inside the rooms;
- Air velocity vectors inside the rooms;
- Temperatures and velocities in the hypocaust;
- Temperatures and velocities inside the chimneys;
- Distribution of gases inside the hypocaust;
- Air flow through the furnace mouth;
- Particles or tracer to confirm air distribution in the hypocaust;
- Air temperatures in the hot room every 40 cm;
- Air temperatures in the warm room every 40 cm;
- Floor temperatures in the entrance area for furnace gases;
- Lower temperature of the hypocaust floor;
- Wall temperature of the hot room at different temperatures;
- Temperatures towards the interior of the floor material in the hot room;
- Videos to ascertain the evolution of air flows and temperatures.

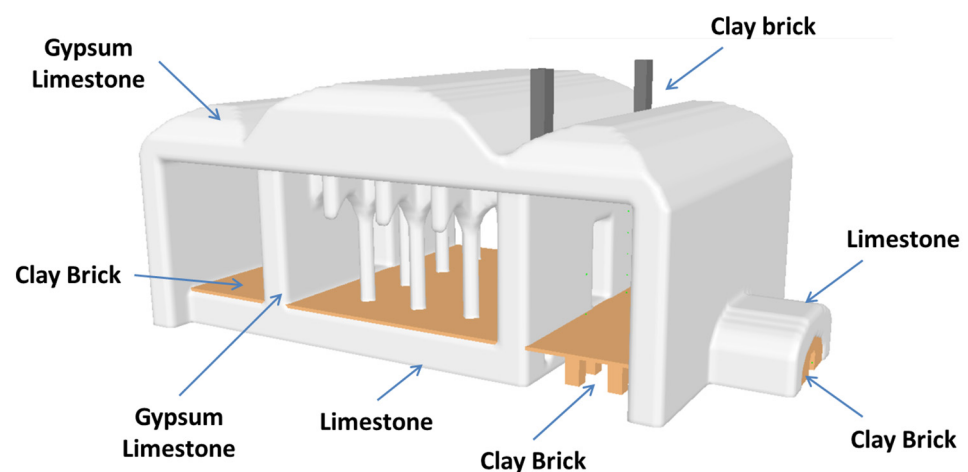


Figure 6. Location of constructive materials.

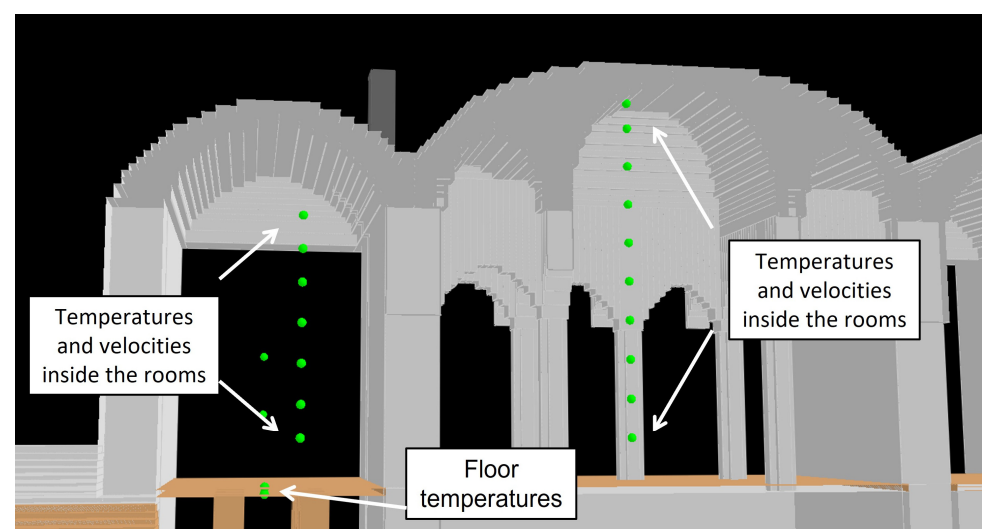


Figure 7. Location of virtual observation points for temperature and velocity inside the rooms of the baths.

3.3. Sensitivity Analysis

The cell size used in a fluid dynamics simulation using finite elements is extremely important, as the precision of the results and the simulation duration and processing time depend upon its dimensions. Other major factors include the amount of data available per surface and volume, as well as the model's adaptation to the building's real geometry. These are all determining factors for ensuring reliable useful results from this research.

In operational terms, two distinct geometries can be identified in this case: the area with high temperatures—including the furnace, hypocaust, and chimneys—and the three rooms (hot, warm, and cold). Heat transfer between these two volumes occurs only through the floor of the hot room, which is also the hypocaust ceiling.

The behaviour of the flow of the hot gases differs greatly between the two volumes, and could have different cell sizes, as low temperatures, slow flows, and simple geometries can be combined with larger cell sizes. In contrast, in order to obtain results with high precision, very hot gases at high speeds with more complex geometries require smaller cell sizes.

For the simulations of the baths in Granada, a single cell size was selected to complete the simulation, as the use of two different-sized cells with complex geometries was incompatible with the model used.

The use of a very small cell is not considered to be of critical importance, as the combustion zone or heat generation source used is a programmable surface, where the Heat Release Rate is the parameter controlled for on each surface unit. If the combustion modelled had been for a fuel defined according to all the thermal reaction parameters, a sensitivity analysis would have been considered essential.

Therefore, the cell size was determined according to the criterion of geometrical precision. Using the measurements provided by the architects guaranteed a sufficiently detailed reconstruction, especially of the hot zone of the furnace and chimneys, with the largest cell size possible. Special care must be taken when using cubic or cuboid cells to model circular sections, such as the furnace vault and the gas collection system of the hypocaust, as the dimensions of these elements should be increased to prevent the existing edges from interfering with the real laminar flows.

As the hypocaust room and chimneys are considered critical zones due to their high temperatures and flow velocities, the cell measurement used is the same as that for the upper rooms. This simplifies the model, validating the size to suit the climatized rooms, where the temperatures and flow velocities are lower.

According to the plans provided, the proposed section for the chimneys was $32 \times 24 \text{ cm}^2$. Therefore, a $30 \times 20 \text{ cm}^2$ model was created, as the slightly smaller section would help confirm the accuracy of the architects' proposal, if the model functioned correctly.

The collection systems or exit zones for the hypocaust fumes were designed with no edges to ensure minimal opposition to the flow of smoke.

It can, therefore, be concluded that 10 cm cubic cells are the largest possible cell size for accurately reproducing these geometries.

4. Discussion and Results

After reproducing the geometry, and entering the parameters for the materials, the dimensions of the ducts, and the openings of the light shafts, doors, and furnace mouths into the computer model, three hypotheses were calculated in order to reach our conclusions on the operation of the baths.

4.1. Operation of the Hypocaust

The first objective is to verify the efficiency of the furnace and hypocaust and their capacity to transmit heat towards the interior of the hot room. The pipes connecting the hypocaust to the exterior (two chimneys), the light shafts in the room vaults, and the openings connecting the hot and warm rooms are, therefore, all taken into account. A distinction is made between the light shafts and the door openings, since they transmit the

heat generated by the radiation and convection of air inside the rooms when the baths are in use. However, the closed system made up of the furnace, hypocaust, and two chimneys set into the walls prevents the transmission of combustion gases and fumes into the room, potentially preventing CO and CO₂ intoxication (Figure 8a,b).

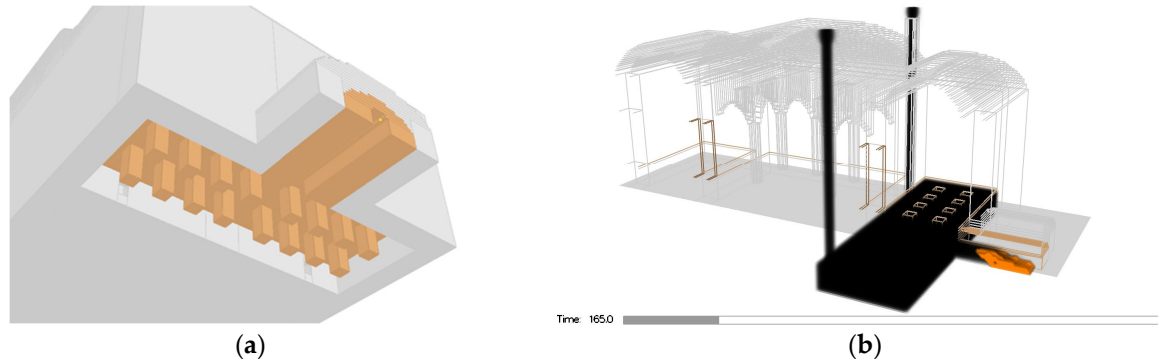


Figure 8. (a) Geometry of the hypocaust space and (b) diagram of the circuit generated by the hypocaust furnace and evacuation chimneys.

In order to confirm the operation of the installation, a sequence of ignition—extinguishing—ignition is simulated, while observing the response of some of the parameters being tested. The initial ignition sequence can take up to 4530 s at the start, when the fire is completely extinguished before being lit again 7000 s later. This then provides information on how long heat is distributed throughout the rooms when the fire is not lit.

There is a stable air entry flow of approximately 0.9 m³/s through the mouth of the furnaces. In the first few seconds, the flow is inverted and smoke is expelled in the opposite direction until the hot gases rise up the chimneys and the flow is inverted inwards once again.

The air entering through the mouth of the furnace is violently mixed with the gases resulting from combustion and, as a result, air entering the hypocaust is heated if its temperature is below that of the fire gases. This also means that in the furnace the flames are guided inwards without directly reaching the upper section of the furnace duct, causing less deterioration to the area (Figure 9).

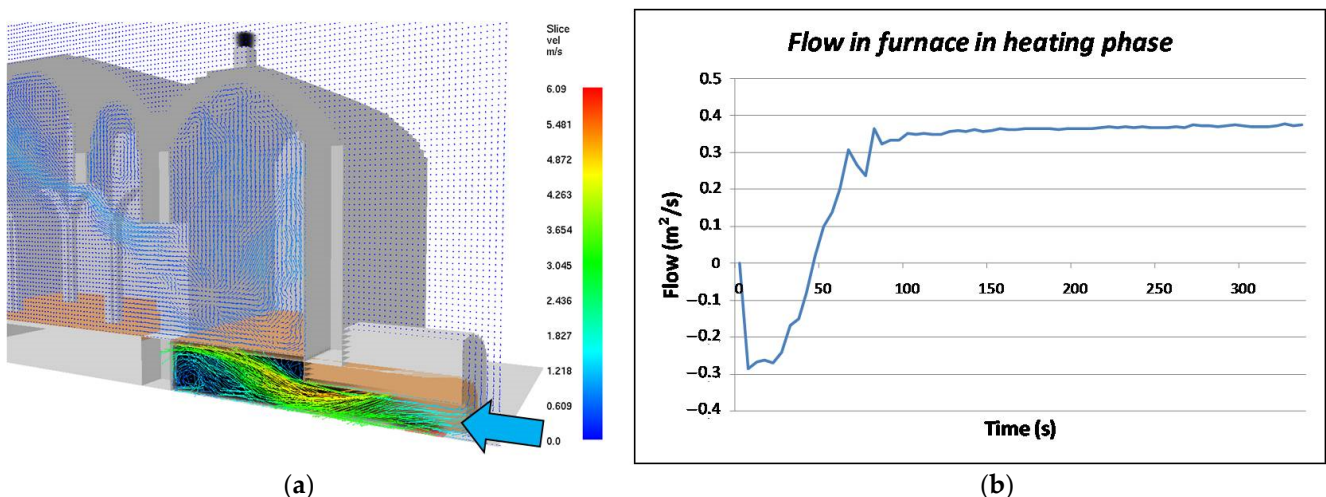


Figure 9. (a) Direction of the entry flow through the mouth of the furnace and (b) time and flow diagram of the mouth of the furnace.

Based on the above, the positioning and size of the openings for expelling smoke from the hypocaust is efficient, given that the hot air distribution results in uniform temperature ranges on the floor of the hot room (Figure 10) (Video S1).

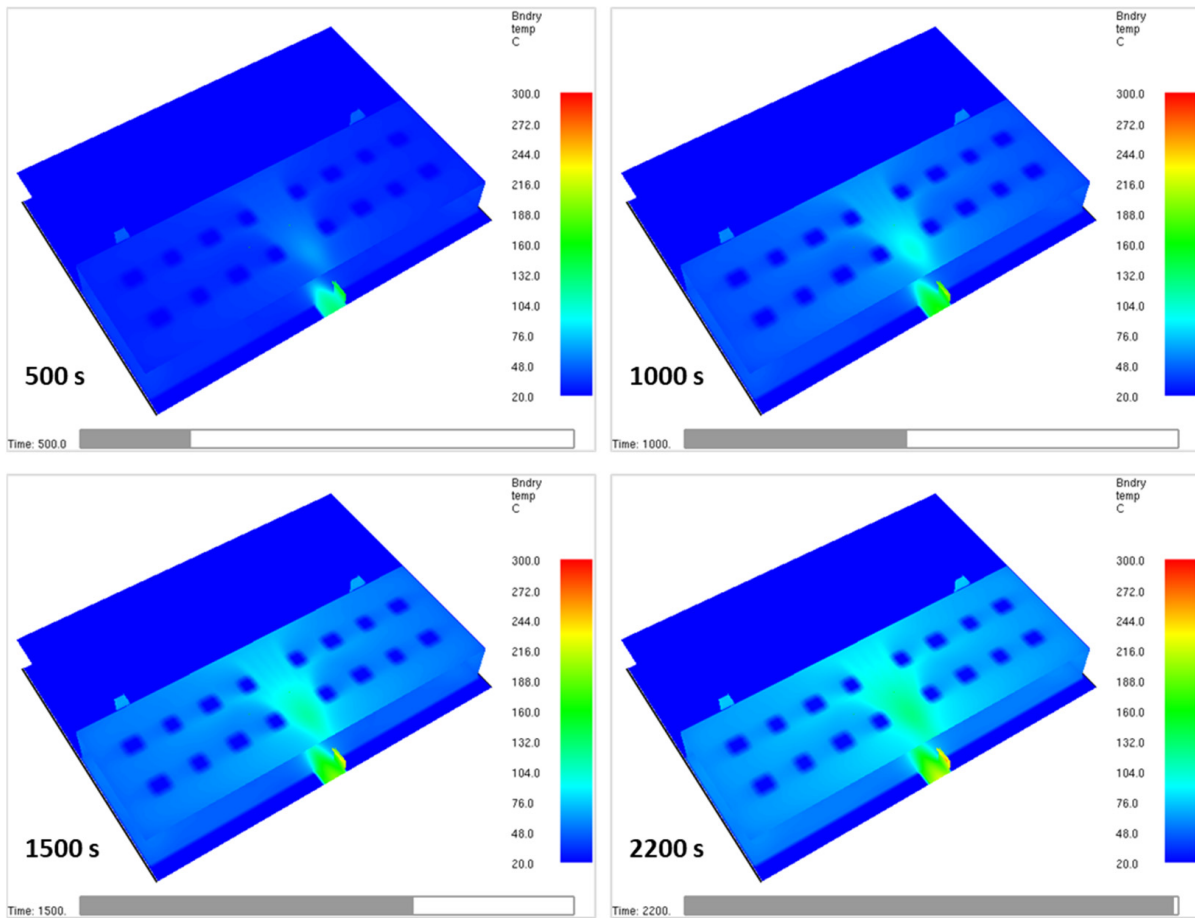


Figure 10. Relatively uniform temperatures on the floor of the hot room were obtained in the first 30 min.

Furthermore, as the height of the opening of the chimneys is lower than the highest point of the furnace, natural air circulation occurs. The gas circulation velocity leads to optimal evacuation, heating the materials, and transmitting heat into the rooms. Finally, the time needed to heat the floor of the hypocaust and the temperature at which it stabilises is verified (Figure 11) (Video S2).

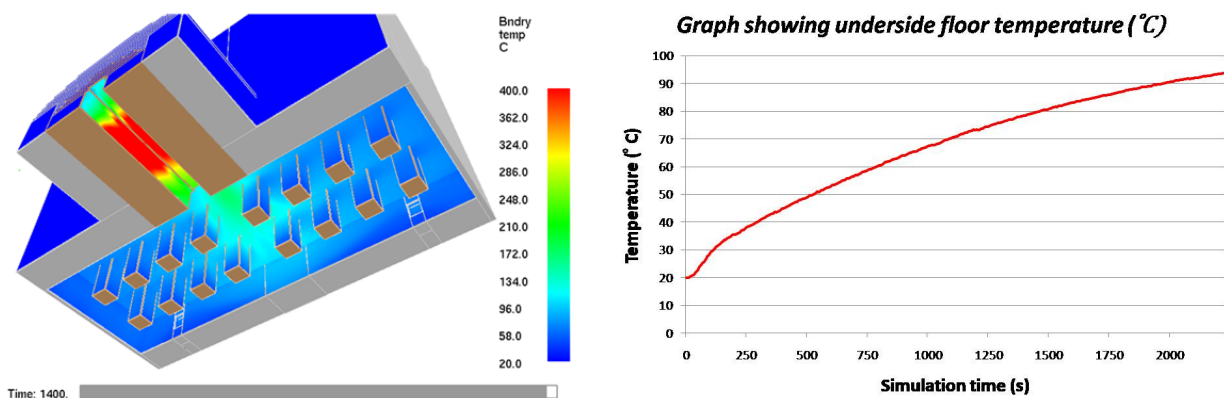


Figure 11. Graph showing floor temperature, which stabilises 30 min (1800 s) after ignition.

The light shafts in the vaults were designed to provide lighting during operation when the hot room is closed. When open, they cause rapid cooling in the rooms, preventing optimal thermal efficiency and, ultimately, wasting energy (Figure 12) (Videos S3 and S4).

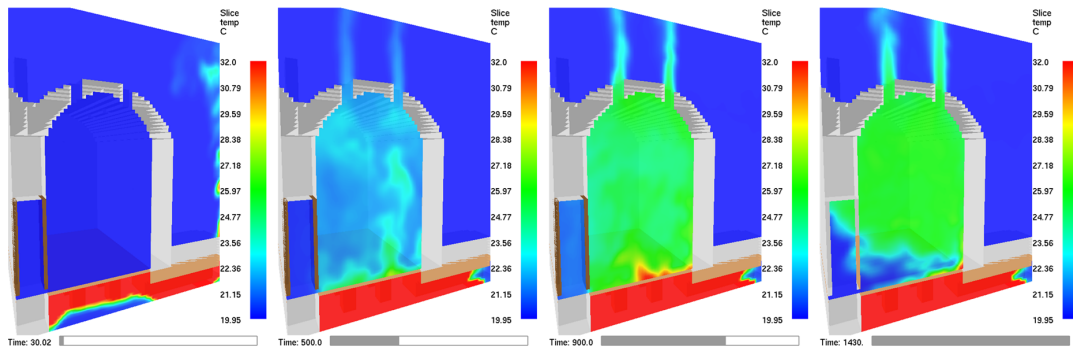


Figure 12. Evolution of interior temperature depending on the opening of the light shafts.

It is confirmed that hot air is distributed evenly upwards in the hot room (Figure 13).



Figure 13. Isosurface with air flow temperatures above 30 °C.

Moreover, the warm room is heated through air circulation that occurs by opening the doors which connect the rooms, so that significant values can be obtained without the need for a hypocaust (Figure 14) (Videos S5 and S6).

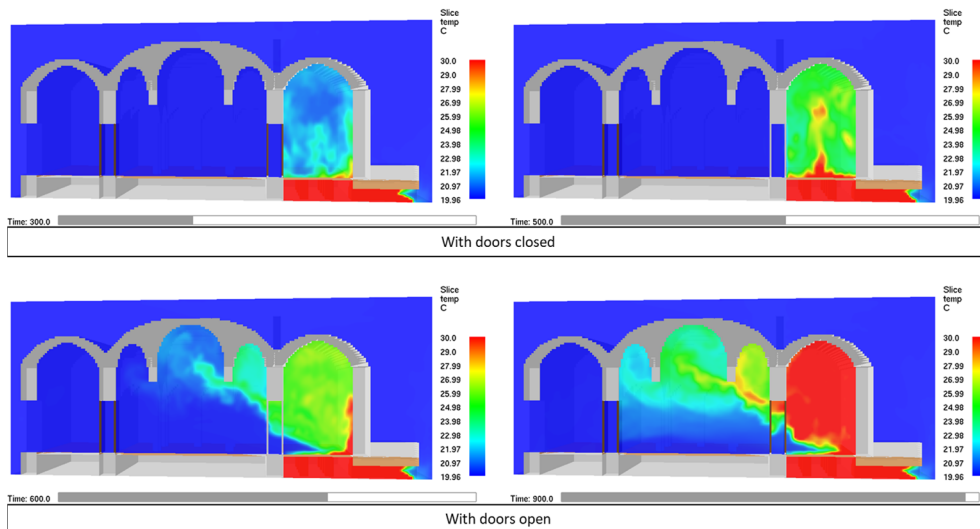


Figure 14. Evolution of interior hot air with doors closed or open.

When the furnace is first lit, the circulation flow is inverted in the first few minutes, moving outwards from the furnace, as not all the air between the furnace and the chimney outlet is heated. According to the laws and principles of thermodynamics, the circulation of cold-to-hot air inside the chimney before being expelled results in a reduction in den-

sity. This circulation allows cold air to enter through the mouth of the furnace, which is heated when it moves above the flames, directing them inwards and preventing them from reaching the brick vault. This substantially increases the air temperature and results in the optimal combustion of the wood, producing hardly any smoke or ash (Figure 15).

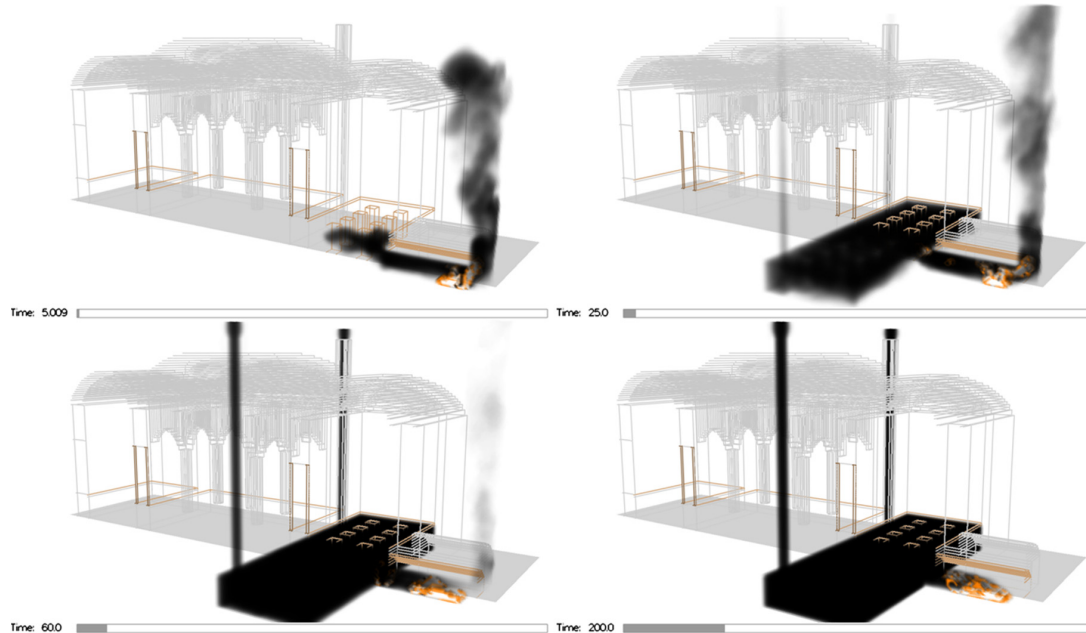


Figure 15. Evolution of gases from the initial stages of ignition until correct circulation is obtained.

While the radiation remains constant for a few minutes after the furnace starts to heat up, the heat transfer or conduction progressively decreases as the interior surfaces (furnace, hypocaust, and chimneys) increase in temperature. Heat conduction across the walls is stabilised as they increase in temperature and the gas gradient decreases. By the end of the simulation, at around minute 40, heat conduction is stabilised.

Convection achieves the opposite effect. As the wall temperatures increase, allowing the gas energy to be maintained, floatability and convection also increase.

During the first two minutes, a transitional phase is observed where air flows in through the furnace mouth and hot gas is expelled through the chimneys.

According to this analysis, the system displays optimal behaviour during the advanced operation phases of the installation, with the thermal transfer balance remaining stable (Figures 16 and 17).

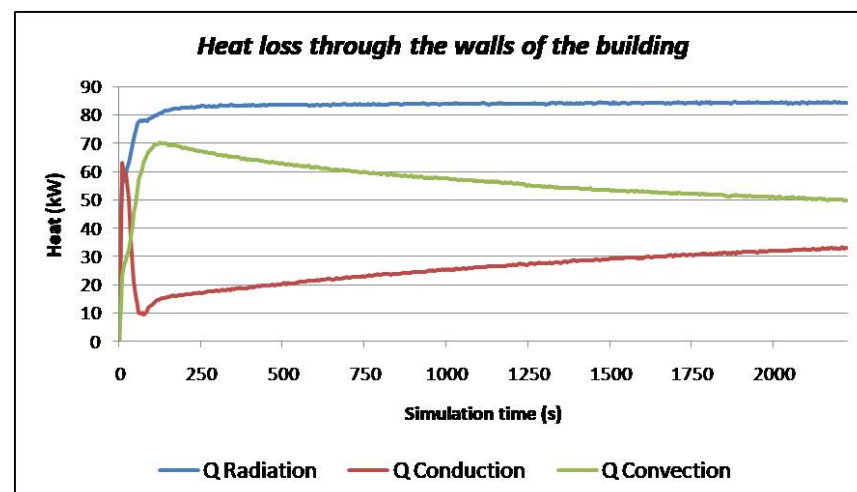


Figure 16. Heat loss through the walls of the building.

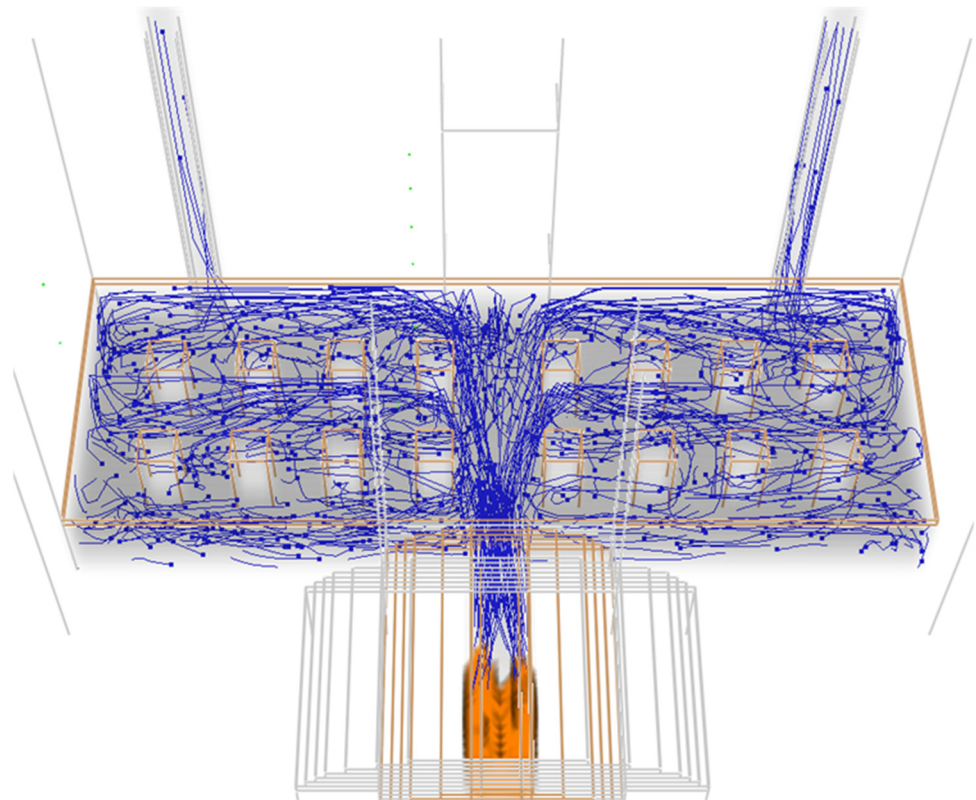


Figure 17. Tracer lines show the distribution of hot gases entering the hypocaust. No areas without hot air access are observed.

4.2. Furnace Power and Temperatures Reached Inside

The following hypothesis focuses on the ability to determine the thermal load needed to ensure a specific range of temperatures inside the hot room.

Firstly, the furnace power required to ensure a suitable temperature on the floor of the hot room is studied. Three different power values in the furnace are analysed, using three simulations with heat emission rates of 100, 160, and 200 kW (Figure 18).

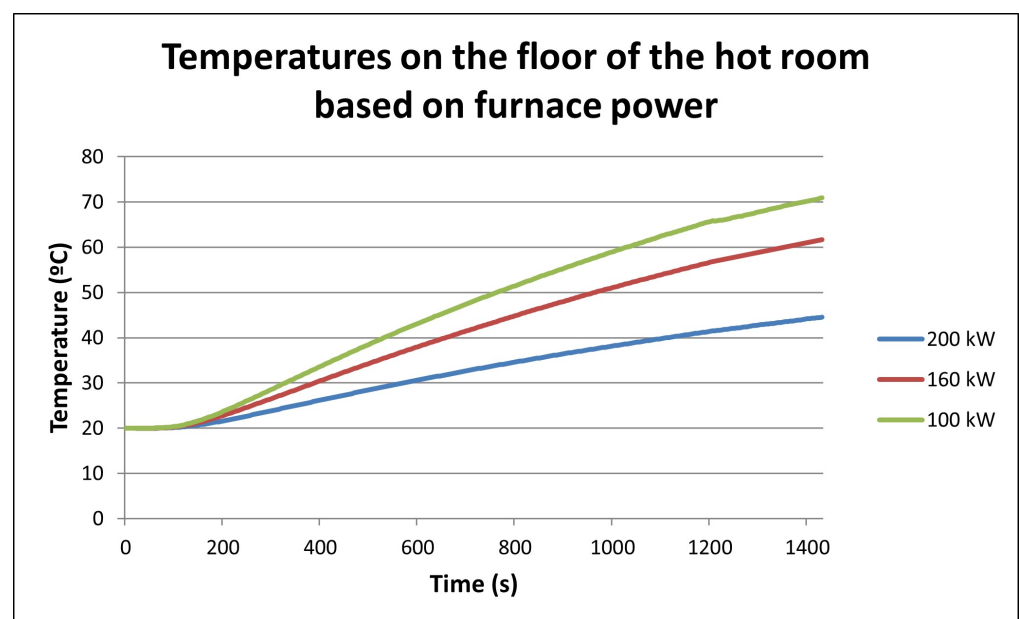


Figure 18. Temperatures on the floor of the hot room based on furnace power.

The values obtained show that with 100 kW power in the furnace, the floor temperature in the hot room is around 40–45 °C. This power is equivalent to the consumption of 22.5 kg of wood per hour.

With 200 kW power, the floor temperature greatly exceeds 70 °C and is, therefore, considered higher than desirable. This power is equivalent to the consumption of 45 kg/h of wood.

Finally, an intermediate power of 160 kW results in temperatures slightly above 60 °C, equivalent to wood consumption of 36 kg/h.

4.3. Utility of the Light Shafts

In the first hypothesis, keeping the light shafts completely open results in some loss of interior heat. In that case, a vector plan for gas velocity, air circulation, and direction can be observed at all times, showing that cold air enters through the light shafts at the ends and hot air exits through those in the centre. Once lit, and until a constant temperature is reached, there are fluctuations and the turbulent movement of the interior air, although no clear flow is established to help optimise the heating of the room. Nevertheless, the optimal temperature is reached after some time, although the energy consumption is higher (Figures 19 and 20) (Video S7).

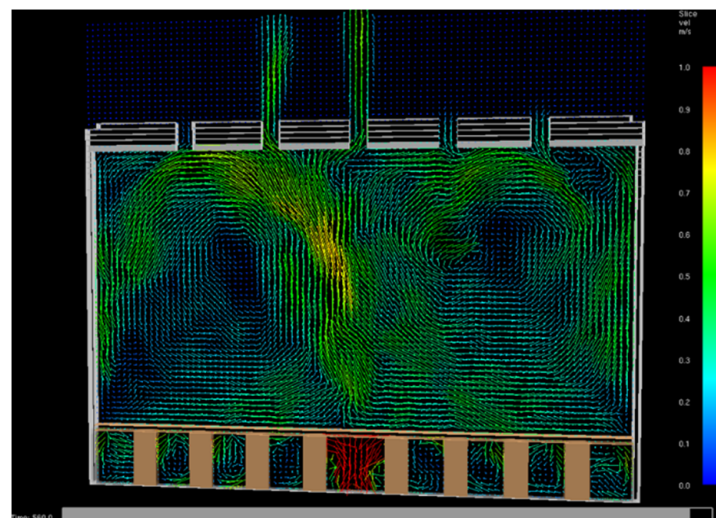


Figure 19. Interior circulation of air. A vector plan for gas velocity and direction.

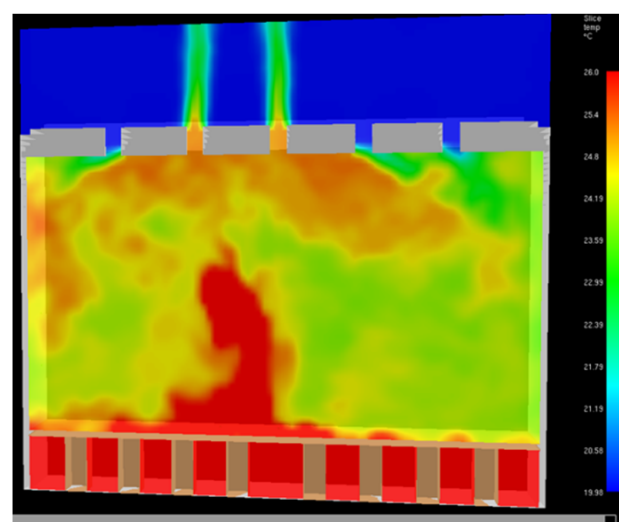


Figure 20. Interior circulation of air. The entry of cold air is observed in the light shafts closest to the perimeter, and exits through the central ones.

5. Conclusions

The Arab baths studied achieve maximum efficiency with the minimum installations possible. The two chimneys are enough to evacuate smoke from a fire with a heat emission rate of up to 500 kW. The temperature in the hot room is regulated by increasing the amount of fuel (wood) in the furnace. The process of lighting and starting the fire lasts between 60 and 80 min.

In the warm room, the air temperature can be increased by opening the door to the hot room. There are no uncomfortable draughts at the height of the bathers, and the flows rise as soon as they reach the opening. The temperature can increase by approximately 5 °C within a few seconds.

In warm areas, such as Granada, a single room with a furnace and hypocaust can be heated, ensuring suitable climate control. An amount of 250 kW power is enough to heat the floor to almost 100 °C and to heat a water heater. The installation supplies this power (0.12 kg/kwh) with 30 kg/hour of wood.

It was also observed that a 1.5 m–2 m high chimney with a 30 × 20 cm section performed very well. The duct section of the furnace is very efficient for the power required. If this section were any wider or longer, the correct heat transfer from the fire gases to the circulating air would not be possible.

The results of this research, based on a hypothetical architectural model, also take into account the limitations of a focus on the correct consideration of the thicknesses and thermal conductivity values of the individual layers of material which make up the building.

Future research should develop a cell with smaller dimensions in order to reduce the errors of the current calculations, and to provide an approximation, with greater certainty, of the result seen over 500 years ago.

Thanks to this study, many hitherto unknown aspects of the operation of this type of historic bath are now known. Hypotheses about the duration of usage, the consumption of wood as fuel, and the temperatures obtained in individual rooms have also been confirmed. In addition, the research carried out shows that the objective of energy efficiency was so desired that the building design and construction were adapted to ensure the greatest possible savings of fuel, and the best use and distribution of heat in the rooms. Proof of this can be found in the precision of the measurements of the mouth of the furnace, the internal space of the conduits, and the distribution of the brick columns in the hypocaust.

These data have resolved the need for the historical and architectural knowledge of these buildings, which were widely found in Spain during the Andalusí era and are still used in many Arab countries, and generally maintain the thermal and hydric concepts similar to those of the baths described here. Although the progression of thermal baths has followed the characteristics of the eras they were built in, as many of them are no longer devoted to their original use, this study provides an overview of the use of heat and heating in the rooms of these baths, enabling a comparison with current baths.

Supplementary Materials: The following supporting information can be downloaded at: <https://www.mdpi.com/article/10.3390/buildings14010039/s1>, Video S1: Sequence of temperature acquisition in the hot room floor, Video S2: Vectors of the circulation of hot air in the hypocaust, Video S3: Hot room flow and temperatures with and without door openings, Video S4: Flows and temperature with and without doors, Video S5: Flows and temperature of the longitudinal section of the baths, Video S6: Vector distribution of the longitudinal section of the baths, Video S7: Temperature flows in the hot room.

Author Contributions: Conceptualization, F.V.L.-M. and C.M.; methodology, S.T.E., E.L.-O.B., F.V.L.-M. and C.M.; validation, S.T.E., E.L.-O.B., F.V.L.-M. and C.M.; investigation, F.V.L.-M. and C.M.; resources, S.T.E. and E.L.-O.B.; data curation, S.T.E. and E.L.-O.B.; writing—original draft preparation, S.T.E., E.L.-O.B., F.V.L.-M. and C.M.; writing—review and editing, S.T.E. and F.V.L.-M.; visualization, S.T.E. and E.L.-O.B.; supervision, F.V.L.-M.; funding acquisition, F.V.L.-M. and C.M. All authors have read and agreed to the published version of the manuscript.

Funding: This research is the result of a commission from the Patronato de la Alhambra y Generalife awarded to professors Camilla Mileto and Fernando Vegas from the Universitat Politècnica de València to work on the “Proyecto de Consolidación del Baño de Hernando de Zafra” (2022–2023). The authors would like to thank the Patronato for their assistance in promoting the knowledge acquired.

Data Availability Statement: The data presented in this study are available on request from the corresponding author. The data are not publicly available due to their ownership.

Acknowledgments: El Patronato de la Alhambra y Generalife, Granada.

Conflicts of Interest: The authors declare no conflict of interest. The funders had no role in the design of the study; in the collection, analyses, or interpretation of data; in the writing of the manuscript; or in the decision to publish the results.

References

1. Free Downloads and Technical Information on Both Programs Can Be Obtained from this Webpage. Available online: <https://pages.nist.gov/fds-smv/index.html> (accessed on 12 February 2023).
2. Qi, D.; Yang, S.; Shu, C.; Zhang, X.; Wang, L.L.; Athienitis, A. Un estudio exploratorio sobre túneles de carretera con marquesina fotovoltaica semitransparente: Desde la perspectiva del ahorro de energía y la seguridad contra incendios. *Construir. Simultáneo*. **2021**, *15*, 537–548. [[CrossRef](#)]
3. Dufour, A. Simulación Mediante la Mecánica Computacional de Fluidos de Escenarios de Incendios Reales en Recintos Industriales. Ph.D. Thesis, Escuela Técnica Superior de Ingenieros de Barcelona, UPC, Barcelona, Spain, 2006.
4. Gagliano, A.; Liuzzo, M.; Margani, G.; Pettinato, W. Thermo-hygro-metric behaviour of Roman thermal buildings: The Indirizzo Baths of Catania (Sicily). *Energy Build.* **2017**, *138*, 704–715. [[CrossRef](#)]
5. Basaran, T.; Ilken, Z. Thermal analysis of the heating system of the Small Bath in ancient Phaselis. *Energy Build.* **1998**, *27*, 1–11. [[CrossRef](#)]
6. Potier, S.; Maltret, J.L.; Zoller, J. Computer graphics: Assistance for archaeological hypotheses. *Autom. Constr.* **2000**, *9*, 117–128. [[CrossRef](#)]
7. Orehounig, K.; Mahdavi, A. Energy performance of traditional bath buildings. *Energy Build.* **2011**, *43*, 2442–2448. [[CrossRef](#)]
8. Oetelaar, T.; Johnston, C.; Wood, D.; Hughes, L.; Humphrey, J. A computational investigation of a room heated by subcutaneous convection—A case study of a replica Roman bath. *Energy Build.* **2013**, *63*, 59–66. [[CrossRef](#)]
9. Oetelaar, T. CFD, thermal environments, and cultural heritage: Two case studies of Roman baths. In Proceedings of the 2016 IEEE 16th International Conference on Environment and Electrical Engineering (EEEIC), Florence, Italy, 7–10 June 2016; pp. 1–6. [[CrossRef](#)]
10. Maragkos, G.; Beji, T. Review of Convective Heat Transfer Modelling in CFD Simulations of Fire-Driven Flows. *Appl. Sci.* **2021**, *11*, 5240. [[CrossRef](#)]
11. Bueno Arcos, J.C. Analysis of Ventilation Effect on Fires Occurred in Industrial Warehouses Using FDS Simulation Tool. Master’s Thesis, Màster Universitari en Ingenieria Química. Universitat Politècnica de Catalunya, Barcelona, Spain, 2018.
12. Also-Moya, J.; Paya-Zaforteza, I.; Hospitaler Pérez, A.; Loma-Ossorio, E. Valencia bridge fire tests: Validation of simplified and advanced numerical approaches to model bridge fire scenarios. *Adv. Eng. Softw.* **2019**, *128*, 55–68. [[CrossRef](#)]
13. Villanueva Rico, M.C. *Casas, Mezquitas y Tiendas de los Hábites de las Iglesias de Granada*; Instituto Hispano-Árabe de Cultura: Madrid, Spain, 1966.
14. Jiménez Serrano, J. *Manual del Artista y del Viajero en Granada*; Don Quijote: Granada, Spain, 1846.
15. Gallego Burín, A. *Granada. Guía Artística e Histórica de la Ciudad*; Editorial Don Quijote: Granada, Spain, 1982.
16. Cuerva, S.; Ángel, M. *El baño de la Puerta de Elvira, de Hernando de Zafra o Casa de las Tumbas*; Estudio Histórico, Estudio Inédito: Granada, Spain, 2002.
17. Malpica Cuello, A. *Granada, Ciudad Islámica. Mitos y Realidades*; Asukaria Mediterránea: Granada, Spain, 1998.
18. Esteban, E.; Aramayo, A.; Cardón, L. Implementación de modelos de turbulencia tipo LES (large eddy simulation) a una cavidad calentada por debajo. In *Mecánica Computacional*; Dvorkin, E., Storti, M.G.Y.M., Eds.; AMCA: Santa Fe, NM, USA, 2010; Volume XXIX, pp. 5537–5549.
19. McGrattan, K.; Hostikka, S.; Floyd, J.; McDermott, R.; Vanella, M.; Mueller, E. *Fire Dynamics Simulator. Technical Reference Guide. Volume 2: Verification*, 6th ed.; NIST Special Publication 1018-2; National Institute of Standards and Technology (NIST), U.S. Department of Commerce: Gaithersburg, MA, USA, 2021. [[CrossRef](#)]
20. McGrattan, K.; Hostikka, S.; Floyd, J.; McDermott, R.; Vanella, M.; Mueller, E. *Fire Dynamics Simulator. Technical Reference Guide. Volume 3: Validation*, 6th ed.; NIST Special Publication 1018-2; National Institute of Standards and Technology (NIST), U.S. Department of Commerce: Gaithersburg, MA, USA, 2021.
21. Chi, J.-H. Using FDS program and an evacuation test to develop hotel fire safety strategy. *J. Chin. Inst. Eng.* **2014**, *37*, 288–299. [[CrossRef](#)]

22. Shu, C.; Wang, L.L. Smoke Spreading Simulation of High-Rise Office Building Based on Evacuation Analysis. In *Environmental Science and Engineering, Proceedings of the 5th International Conference on Building Energy and Environment, COBEE 2022, Montréal, QC, Canada, 25–29 July 2022*; Springer: Singapore, 2022. [[CrossRef](#)]
23. Tormo, S. *Funcionalidad Hídrica y Térmica de los Complejos Termas Romanos*; Generalitat Valenciana, Las Termas Mayores de Mura en Llíria: Valencia, Spain, 2021; ISBN 978-84-482-6533-5.

Disclaimer/Publisher’s Note: The statements, opinions and data contained in all publications are solely those of the individual author(s) and contributor(s) and not of MDPI and/or the editor(s). MDPI and/or the editor(s) disclaim responsibility for any injury to people or property resulting from any ideas, methods, instructions or products referred to in the content.